Journal of Computers Vol. 31 No. 5, 2020, pp. 146-158
doi:10.3966/199115992020103105011

A Comparative Analysis Between IFS-based and Non-IFS-based Classification on Color Texture

Chih Ping Yen*, Cheng Tan Tung

Department of Information Management, Central Police University, Taoyuan 33304, Taiwan
{peter, tung}@mail.cpu.edu.tw

Received 20 April 2019; Revised 15 August 2019; Accepted 11 October 2019

Abstract. Color texture classification plays an important role in computer vision and has a wide variety of applications. Many methods of color texture analysis have been developed over the years; however, a major problem is that textures in the real world are often not uniform owing to variations in rotation and scale. Additionally, color texture images usually contain noises and uncertainties. According to the literature, intuitionistic fuzzy set (IFS) is helpful in modeling vagueness or uncertainty. Therefore, the purpose of this study is to prove that IFS will be a good approach to improve the classification performance of color texture. We applied six well-known texture descriptors (i.e. LBP, GLCM, LTP, LDiP, LDeP and LTrP) to compare them based on IFS and non-IFS based methods, respectively. Experiments show that the IFS-based method can improve the accuracy by 0.88% to 13.16% compared with the non-IFS-based method. In addition, IFS-based methods are also more robust than non-IFS based on rotation and scaling. This conclusion can be used by texture classification researchers to apply IFS to further improve the performance of their own color texture classification methods.

Keywords: GLCM, intuitionistic fuzzy set (IFS), LBP, LDeP, LDiP, LTP, LTrP, texture classification

1 Introduction

This texture is a very important attribute in the field of computer vision, and many methods of color texture analysis have been developed over the years. These methods can be broadly divided into seven classes, such as statistical approaches, structural, transform-based, model-based, graph-based, learning-based, and entropy-based approaches. Among all classes, statistical methods are the most popular because of its good discrimination, efficiency, robustness and so on. [1]. For statistical methods, the statistical properties of the grayscale spatial distribution are used as texture descriptors. However, color texture images are often described by color models such as RGB, HSV, and L*a*b. That is to say, all color texture images must undergo the pre-processing of gray level space conversion. Because this image pre-processing process will cause the loss of texture information, it directly affects the performance of texture classification. The motivation of this study is how to avoid the loss of image information caused by previous processing, and thus improve the texture classification performance of such statistical methods.

Intuitionistic fuzzy set (IFS) theory [2] is an extension of fuzzy set (FS). It is employed in image processing to enhance images when recovering important structures that are not properly visible. However, it has only been demonstrated in the contexts of contrast enhancement, edge detection, segmentation, clustering and fusion; in each case, it has been observed to significantly improve performance [3-5]. Therefore, this article conducts a pilot study on the classification of color texture based on IFS. We try to use some statistical texture classification methods, such as LBP, GLCM, LTP, LDiP, LDeP and LTrP. Then apply IFS for image pre-processing and use the proposed simple measure of similarity for comparison. The well-known color texture database CBT is used in this study. Experimental results have proven that using IFS can significantly improve the accuracy of the texture classification method and obtain better robustness than non-IFS.

The rest of this paper is organized as follows. In the next section, briefly introduces statistical texture classification. Section 3 describes how intuitionistic fuzzy sets are applied to images. Section 4 presents

* Corresponding Author

the proposed measure of similarity between two IFSs. Sections 5 and 6 analyze performance and robustness on IFS-based and non-IFS-based, respectively. Finally, Section 7 concludes the whole paper.

2 Statistical Texture Classification

Texture is defined as spatially homogenous and has repeated visual patterns, which is an important characteristic for analyzing image types that involve image processing, pattern recognition, and computer vision; this characteristic has applications for medical image analysis, remote sensing data, object recognition, industrial surface inspection, document segmentation, and content-based image retrieval [6]. Texture classification aims to assign texture labels to unknown textures according to training samples and classification rules. During the last three decades, numerous methods have been proposed for image texture classification or retrieval. As mentioned in the previous section, these methods can be divided into seven categories, among which statistical texture classification is the most popular because of its good discrimination, robustness and so on. In statistical methods, gray level co-occurrence matrix (GLCM) and local binary pattern (LBP) are the most classical and mainstream methods, and each of them extends a number of different approaches. This study selected six well-known texture descriptors as the object of comparative analysis, namely LBP, GLCM, LTP, LDiP, LDeP and LTrP.

2.1 Gray Level Co-occurrence Matrix (GLCM)

GLCM introduced by Haralick [7] attempt to describe texture by statistically sampling how certain grey levels occur in relation to other grey levels. The advantages of GLCM are that it is easy to implement and it gives an exact image texture. However, GLCM also has several drawbacks: the process of computing GLCM is complex, and computing the 14 typical texture parameters will take a long time—especially for large images—thus limiting its capability to capture texture information at multiple scales while maintaining sensitivity to noise. Because of this, GLCM methodology has always been developed with large numbers of variations designed to improve its drawbacks. Siqueira and colleagues [8] presented a novel strategy for extending GLCM to multiple scales through two different approaches: a Gaussian scale-space representation and an image pyramid (which is defined by sampling the image both in space and scale). Kim and colleagues [9] proposed the fractal dimension co-occurrence matrix (FDCM) method, incorporating both fractal dimension and GLCM method. Mamat et al. [10] proposed an extracting local Haralick's texture feature based on a predetermined region using the color co-occurrence matrix method for local texture information.

2.2 Local Binary Pattern (LBP)

LBP is the classic method after GLCM, first proposed by Ojala and colleagues [11], which labels the pixels of an image by thresholding the 3×3 neighborhood of each pixel and considers the result as a binary number. Since the LBP method combines structural and statistical features to improve the performance of texture analysis, many LBP-like methods have subsequently been proposed. Tan and Triggs [12] proposed local ternary pattern (LTP), which extends original LBP to 3-valued codes. Jun and colleagues [13] proposed compact LBP (CLBP) by maximizing mutual information between features and class labels; the CLBP provides better classification performance with a smaller number of codes than does original LBP. Jabid and colleagues [14] proposed local directional pattern (LDiP), which computes edge response values by using Kirsch masks in all eight directions at each pixel position and then generates a code from the relative strength magnitude. Zhang and colleagues [15] proposed local derivative pattern (LDeP), which extracts high-order local information by encoding various distinctive spatial relationships contained in a given local region. Murala and colleagues [16] proposed local tetra pattern (LTrP) for content-based image retrieval (CBIR); their proposed method encodes the relationship between the referenced pixel and its neighbors, based on directions that are calculated using the first-order derivatives in vertical and horizontal directions. Dubey [17] developed Local Bit-plane Decoded Pattern (LBDP), which is generated by finding a binary pattern using the difference of center pixel's intensity value with the local bit-plane transformed values for each image pixel. Verma et al. [18] utilized the complementarity of LBP and LNDP (local neighborhood difference pattern), combining to extract the most of the information that can be captured using local intensity differences. Banerjee et al. [19] also

proposed a texture descriptor called local neighborhood intensity pattern (LNIP), which considers the relative intensity difference between a particular pixel and a central pixel by considering its neighbors and generates a sign and a magnitude pattern.

3 Intuitionistic Fuzzy Image

3.1 Intuitionistic Fuzzy Set (IFS)

IFS theory, which is an extension of fuzzy set (FS), enhances images and helps to recover important structures that are not properly visible [3]. Atanassov [2] pioneered construction of IFS, which is defined by three feature functions as the degree of membership, degree of non-membership, and degree of hesitation or uncertainty.

Definition: An IFS A in universe X is an expression given by

$$A = \left\{ x, \mu_A(x), \nu_A(x) \middle| x \in X \right\}, \tag{1}$$

where $\mu_A(x): X \to [0,1]$, $\nu_A(x): X \to [0,1]$ are the membership and non-membership degree of an element x to the set A with the condition:

$$0 \le \mu_A(x) + \nu_A(x) \le 1, \tag{2}$$

for each $x \in X$,

For each IFS in X, we call $\pi_A(x) = 1 - \mu_A(x) - \nu_A(x)$ the degree of hesitancy of x to A, $0 \le \pi_A(x) \le 1$ for each $x \in X$. The illustration of these degrees is shown in Fig. 1.

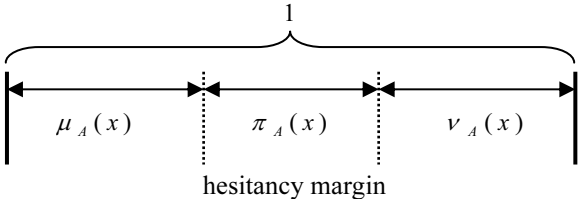

Fig. 1. Relationships between membership, non-membership, and hesitation degrees [17]

IFS is helpful in modeling vagueness or uncertainty, and important applications of IFS have been developed in many diverse areas, including medical diagnosis [20], pattern recognition [21], image processing [22], and decision making [23].

3.2 An Intuitionistic Fuzzy Image is Constructed Using Intuitionistic Fuzzy Generator (IFG)

Suppose image A of size $M \times N$ pixels has L gray levels ranging between 0 and $L-1$. When applying IFS for image processing [24], an image can be considered as an array of fuzzy singletons. An intuitionistic fuzzy image is written as

$$A_{IFS} = \left\{ x, \mu_A(x), \nu_A(x), \pi_A(x) \right\}, \tag{3}$$

for $0 \le x \le$ L-1, where x is the pixel value at (i, j) point, $i = 0, 1, ..., N-1$, $j = 0, 1, ..., M-1$.

With the condition

$$0 \le \mu_A(x) + \nu_A(x) \le 1, \tag{4}$$

then

$$\pi_A(x) = 1 - \mu_A(x) - \nu_A(x), \tag{5}$$

where $\mu_A(x) \to [0,1]$: membership degree; $\nu_A(x) \to [0,1]$: non-membership degree; $\pi_A(x) \to [0,1]$: hesitancy degree.

Vlachos [25] represents the membership degree of image by $\mu_A(x) = (x - x_{\min})/(x_{\max} - x_{\min})$ where

$x_{\max}$ and $x_{\min}$ are the maximum and the minimum gray levels of the image. Sugeno's intuitionistic fuzzy generator (IFG) [26] constructs non-membership degree $\nu_A(x)$ as

$$\nu_A(x) = \frac{1-\mu_A(x)}{1+\lambda\,\mu_A(x)}, \tag{6}$$

where parameter $\lambda > 0$, and hesitancy degree

$$\pi_A(x) = 1-\mu_A(x) - \frac{1-\mu_A(x)}{1+\lambda\,\mu_A(x)}. \tag{7}$$

By varying the $\lambda > 0$ parameter, different intuitionistic fuzzy set can be obtained. As λ is not a fixed value for all images, the optimum value of λ is obtained by maximizing fuzzy entropy. The fuzzy entropy was described in the next subsection.

3.3 Fuzzy Entropy

Information entropy (also called "Shannon's entropy") was first introduced by Shannon [27] to measure the degree of uncertainty that exists in a system. De Luca and Termini [28] were the first to introduce the concept of fuzzy entropy. Let A be a fuzzy set in $X = \{x_1,..., x_n\}$; the entropy $E(A)$ of the fuzzy set is as follows:

$$E(A) = -\frac{1}{n}\sum_{i=1}^{n}[\mu_A(x_i)\log\mu_A(x_i) + (1-\mu_A(x_i))\log(1-\mu_A(x_i))]. \tag{8}$$

This research found the maximizing fuzzy entropy λ according to equation (8) with all 2,800 experimental samples from the Colored Brodatz Texture (CBT) database. The experimental result indicate an approximated maximum entropy value of 4.8342 when λ is 3.6.

3.4 Intuitionistic Fuzzy Image Processing

The HSV color model is widely used in computer graphics, image processing, pattern recognition, and other fields. In this space, color is presented in terms of three components based on cylinder coordinates: hue (H), saturation (S), and value (V). Hue is used to distinguishing colors, saturation is the percentage of white light added to a pure color, and value denotes the brightness perception of a specific color. The advantage of HSV is that each of its attributes corresponds directly to human conceptual understanding of colors, which has the ability to separate chromatic and achromatic components. Besides, the HSV color model gives the best color histogram feature of all color models [29]. The perceived disadvantage of HSV is that the saturation attribute corresponds to tinting; thus, desaturated colors have increased total intensity. Because of its advantages, however, we adopt the HSV color model.

First, the RGB (red, green, and blue) image is converted into an HSV (hue, saturation, and value) image. Then, intuitionistic fuzzy image processing is applied to generate the image's optimal membership degree $\mu(x)$, non-membership degree $\nu(x)$, and hesitancy degree $\pi(x)$ with maximum fuzzy entropy. Since we obtain three $\mu(x)$, three $\nu(x)$, and three $\pi(x)$ for each image (i.e., a total of nine degrees), images have more abundant information for texture classification than they do with other approaches.

Given an example, the image D47 of Colored Brodatz Texture (CBT) database is used for representing intuitionistic fuzzy images. Fig. 2 depicts those images along with their corresponding membership, non-membership and hesitancy components.

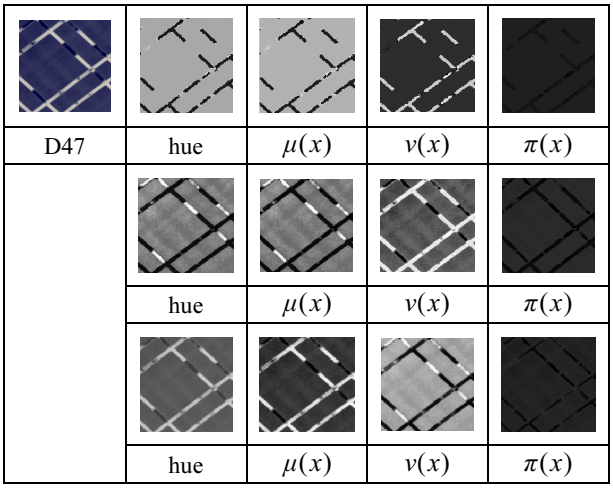

Fig. 2. Image D47 showing corresponding membership, non-membership, and hesitancy components from the CBT database

4 A Simple Measure of Similarity Between Two IFSs

Many measures of similarity between fuzzy sets have been proposed and researched over the past two decades. Szmidt and Kacprzyk [30] introduced the Hamming distance between IFSs. Liang [31] proposed relationships between these similarity measures for IFS with applications to pattern recognition. Furthermore, Mitchell [32] modified Li and Cheng's measures from a statistical viewpoint. Julian and colleagues [33] showed that Mitchell's improvement [32] contained questionable results and then provided some revisions. Pekala and Balicki [34] also proposed similarity measure by using order on interval-valued IFSs connected with lexicographical order.

Besides, a popular quantity used to express the structural similarity is the Root-Mean-Square Distance (RMSD) [35] as

$$RMSD(A,B)=\sqrt{\frac{1}{n}\sum_{i=1}^{n}d(a_i,b_i)^2}\,, \tag{9}$$

where $A=\{a_1,a_2,...,a_n\}$ and $B=\{b_1,b_2,...,b_n\}$ are two sets of points, $d(a_i,b_i)$ is the Euclidian distance between a_i and b_i.

Combining the above views, this paper proposed the following parametric equation

$$D_{IFS}(Q,T)=\sqrt{\frac{\sum_{i=1}^{n}w_i\left(\frac{\left|h_\mu^Q(i)-h_\mu^T(i)\right|+\left|h_\nu^Q(i)-h_\nu^T(i)\right|+\varphi\left|h_\pi^Q(i)-h_\pi^T(i)\right|}{3}\right)^2}{n}}\,, \tag{10}$$

where $D_{IFS}(Q,T)$ is the distance between query image Q and target image T, and $h_\mu^Q(i)$, $h_\nu^Q(i)$, $h_\pi^Q(i)$ and $h_\mu^T(i)$, $h_\nu^T(i)$, $h_\pi^T(i)$ are the histograms of query image Q and target image T at μ, ν, and π images respectively, and n is the bin number of a histogram, w_i is the weight for different bin, and $\varphi \geq 0$ specify the effect of π image. We assign $w_i=1$ and $\varphi=1$ for distance measure between two histograms in the latter experiments. Then, we convert our distance measure into a similarity as

$$S_{IFS}(Q,T)=\frac{1}{1+D_{IFS}(Q,T)}\,, \tag{11}$$

where $0<S_{IFS}(Q,T)\leq 1$ is the similarity of between query image Q and target image T based on IFS.

5 Performance Analysis on IFS-based and Non-IFS-based

In this section, we compare the performance between IFS-based and non-IFS-based methods to six well-known texture descriptors by equation (10) and (11), namely LBP, GLCM, LTP, LDiP, LDeP and LTrP. Table 1 summarizes all the notation of methods with detailed description and feature dimensions based on IFS or non-IFS (i.e., HSV color model) to perform experiments in accuracy.

Table 1. Summary of the six texture classification methods

Method	Notation	Description	Feature dimension
LBP	$LBP_{URI}(HSV)$	The original LBP with rotation invariant uniform patterns, the number of neighbors is 8, and the radius of the circular neighbor is 1.	30
	$LBP_{URI}(IFS)$		90
GLCM	$GLCM\ (HSV)$	The four Haralick's features, Contrast, Correlation, Energy and Homogeneity, are calculated from 36 GLCMs respectively, which d take from 1 to 9, and θ take the four directions value of 0°, 45°, 90° and 135°.	432
	$GLCM\ (IFS)$		1,296
LTP	$LTP\ (HSV)$	Local Ternary Pattern [12] extends original LBP to 3-valued codes.	1,536
	$LTP(IFS)$		4,068
LDiP	$LDiP\ (HSV)$	Local Directional Pattern [14] computes the edge response values by Kirsch masks in all eight directions at each pixel position and generates a code from the relative strength magnitude.	768
	$LDiP\ (IFS)$		2,304
LDeP	$3rd\ order\ LDeP\ (HSV)$	Local Derivative Pattern [15] extract third-order local information by encoding various distinctive spatial relationships contained in a given local region.	3,072
	$3rd\ order\ LDeP\ (IFS)$		9,216
LTrP	$3rd\ order\ LTrP\ (HSV)$	Local Tetra Patterns [16] encodes the relationship between the referenced pixel and its neighbors, based on the directions that are encoded the third-order LTrP in vertical and horizontal directions.	9,984
	$3rd\ order\ LTrP\ (IFS)$		29,952

Experimental data. To validate the performance of IFS-based and non-IFS-based methods, we use the above mentioned CBT database. The CBT consists of 112 periodic or non-periodic 640×640 color texture images, parts of which are shown in Fig. 3. Each color texture image is divided into 25 non-overlapping sub-images for experiments, resulting in 11,200 total samples for size of 128×128 pixels. The size of the texture image is a key factor that affects classification performance.

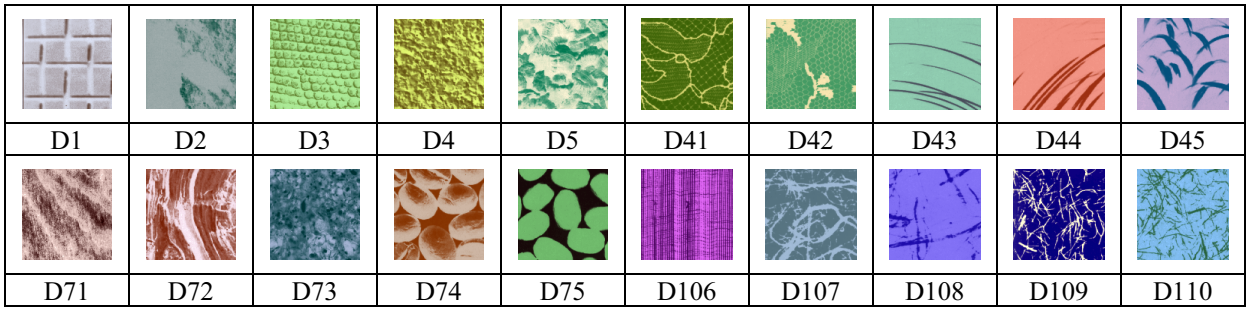

Fig. 3. Samples from the CBT database

Basically, larger sizes tend to provide better performance; however, this does not mean that the bigger the image size, the better the rate of accuracy. According to experimental result, the 128×128 image size has better performance among the 256×256, 128×128, 64×64 and 32×32 size. Small texture image sizes cannot capture large-sized texture structures that may be dominant features, are not very robust against local changes in texture, and are highly sensitive to small variations. Thus, large sizes generate more strongly individualized features while decreasing performance.

Experimental setup. The k-Nearest Neighbor (k-NN) classification is one of the simplest but widely using machine learning algorithm. An object is classified by the distance from its neighbors, with the object being assigned to the class most common amongst its k nearest neighbors. We use 1-NN approach

as a classifier in this work, i.e. the texture image is classified to the class of its nearest neighbor by equation (10) and (11).

The sample data was split into training and test sets using the 25-fold cross-validation method. The 25-fold cross-validation is just the leave-one-out method, for N samples, a total of N trials are conducted. In each trial, a sample is taken out from the data set and kept for testing and the others are used for training. This procedure was repeated for all samples and the accuracy rate obtained as the percentage of classified samples out of the total number of samples. This methodology is superior to random partitioning of data to generate training and test sets as the resultant performance of the system may not reflect its true ability for texture classification. The experiment is implemented in Matlab programming and run on a PC-based machine with an Intel Core i5-3470 CPU, 3.2GHz, and 3.48G RAM.

Experimental results. The graphical analysis of color texture classification for IFS-based and non-IFS-based methods is shown in Fig. 4. It is found that IFS-based methods are significantly more effective classification of color textures than non-IFS-based (i.e., HSV-based) methods. The accuracy is improved from 0.88% to 13.16% as following:

(1) The IFS-based LBP_{URI} works better than the non-IFS-based LBP_{URI} by 0.88%.

(2) The IFS-based GLCM outperforms the non-IFS-based GLCM by 13.16%.

(3) The IFS-based LTP has higher accuracy than the non-IFS-based LTP by 1.12%.

(4) The performance of IFS-based LDiP is enhanced 1.84% comparing with the non-IFS-based LDiP.

(5) The performance of IFS-based 3rd order LDeP is also enhanced 2.61% comparing with the non-IFS-based 3rd order LDeP.

(6) The IFS-based 3rd order LTrP outperforms the non-IFS-based 3rd order LTrP by 3.94%.

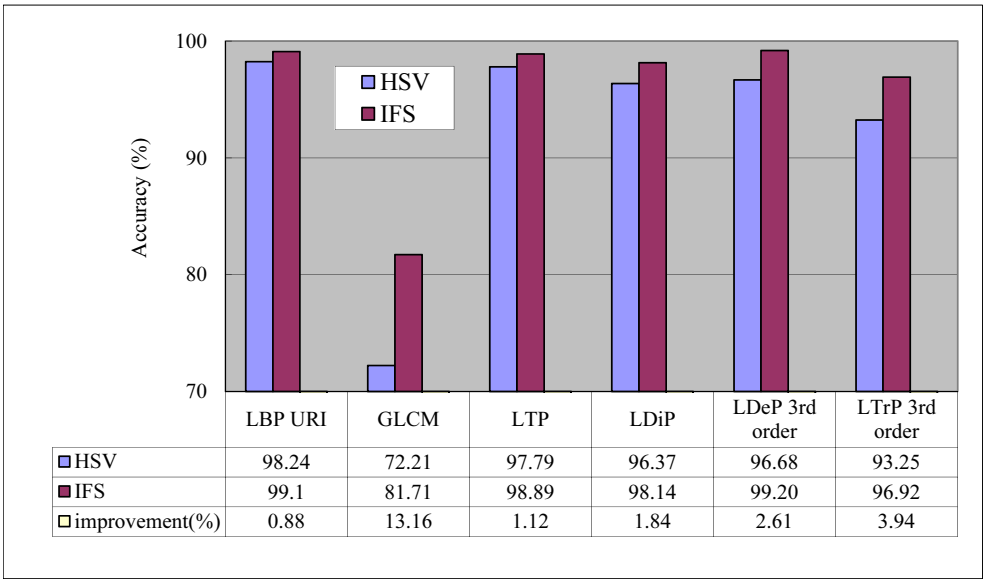

	LBP URI	GLCM	LTP	LDiP	LDeP 3rd order	LTrP 3rd order
HSV	98.24	72.21	97.79	96.37	96.68	93.25
IFS	99.1	81.71	98.89	98.14	99.20	96.92
improvement(%)	0.88	13.16	1.12	1.84	2.61	3.94

Fig. 4. The classification results for IFS-based vs. non-IFS-based (i.e., HSV-based) methods

6 Robustness Analysis on IFS-based and Non-IFS-based

In many real applications, it is very difficult or impossible to ensure that captured images have the same rotations and scales as other images. In following sections, our aim is to evaluate the robustness of IFS-based methods when changes in rotation and scale occur. We use the standard data set as a training set. Thus, the sub-images rotation and scale are the test sets. The experimental results show that IFS-based methods can resist the above-mentioned variations.

6.1 Analysis on Rotation

Experimental data: For the analysis of rotation robustness, all 112 texture images are rotated by 19 different angles (i.e., 0°, 10°, 20°, …, 180°). Here we use the nearest neighbor interpolation method for rotation of image. Each rotated image is divided into four non-overlapping 320×320 sub-images. Four

128×128 sub-images are then cropped from the center of the 320×320 sub-images. Hence, we obtain a rotation test set with a total of 8,512 (=112×19×4) sub-images. Fig. 5 shows an example of different rotation angles from 10 to 180 degrees using 10-degree steps.

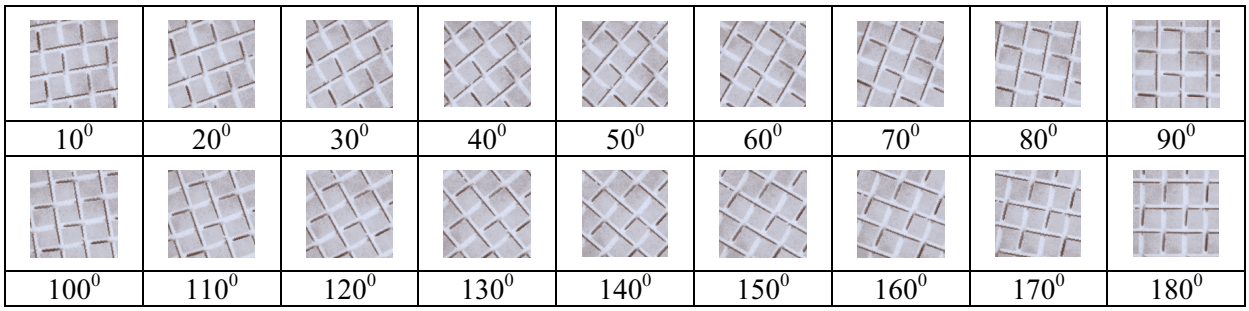

Fig. 5. Rotation angles from 10° to 180° using 10-degree steps for image D01 from the CBT database

Experimental setup: We also use 1-NN approach as a classifier. The sample data was split into training and test sets using the 25-fold cross-validation method.

Experimental results: The results of classification accuracy with respect to rotation factors for six tested methods are shown in Fig. 6 for clear comparison, and we explore the IFS-based methods are more effective classification of color textures than non-IFS-based methods under at each rotation angle. That confirms the robustness of IFS-based methods. In addition, Table 2 represents the average accuracy rate of all rotation angles on the CBT database and the average improvement rate after using IFS. It can be seen from the table that the average improvement rate is significantly increased after using IFS-based method.

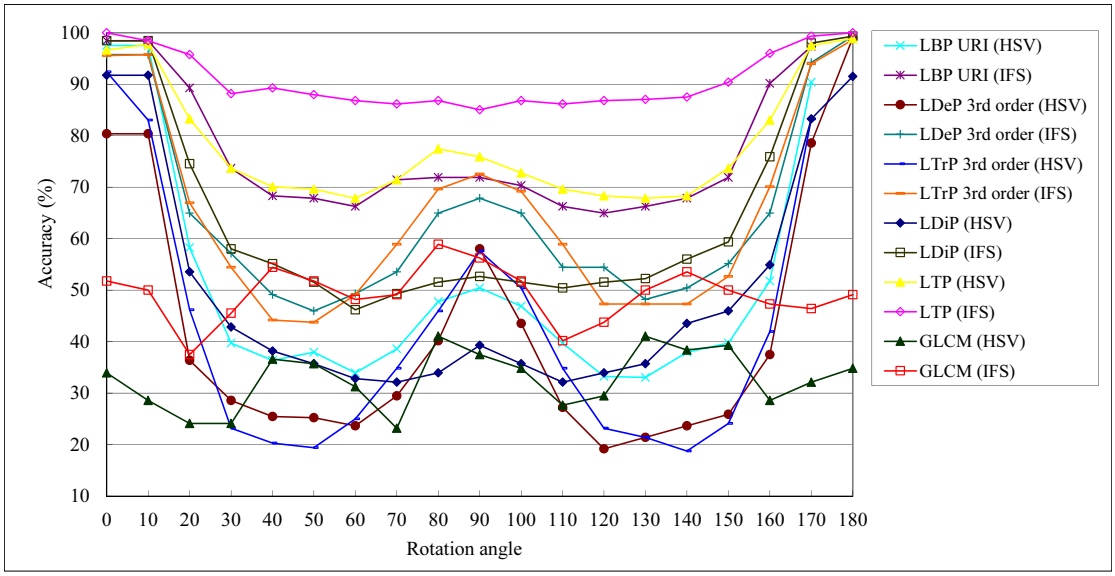

Fig. 6. Texture classification results for six tested methods with IFS-based and non-IFS-based on the rotated CBT database

Table 2. Average accuracy rate of all rotation angles and the average improvement rate after using IFS

Method	LBP		GLCM		LTP		LDiP		LDeP		LTrP	
	HSV	IFS	HSV	IFS	HSV	IFS	HSV	IFS	HSV	IFS	HSV	IFS
Average accuracy rate (%)	52.96	77.48	32.75	49.25	78.09	90.77	49.93	64.76	42.30	64.77	44.29	65.07
Average improvement rate (%)	46.29		50.36		16.23		29.70		53.12		46.92	

Furthermore, the LTrP method in Table 2 has the best average improvement rate, and uses the red line in Fig. 7 to show its accuracy improvement rate after using IFS at each rotation angle. We can see that there is significant improvement to gain at certain rotation angles. Besides, we also summarize the accuracy above 90% for six tested methods. It is found that IFS-based methods still can improve the accuracy from 0.34% to 8.53% even under high accuracy. The average improvement rate of accuracy can reach 3.28%.

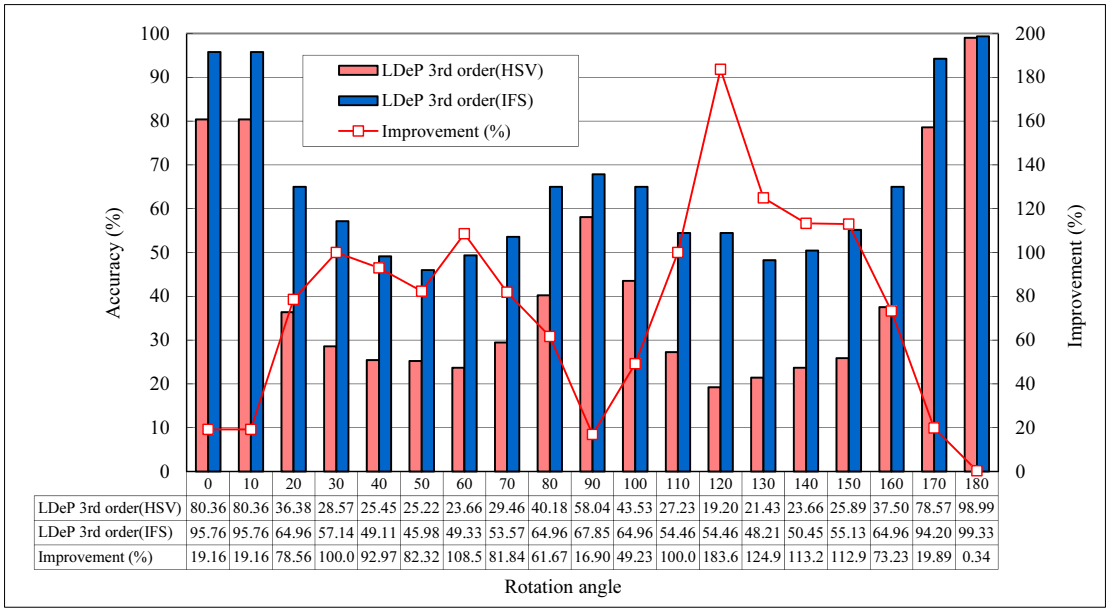

	0	10	20	30	40	50	60	70	80	90	100	110	120	130	140	150	160	170	180
LDeP 3rd order(HSV)	80.36	80.36	36.38	28.57	25.45	25.22	23.66	29.46	40.18	58.04	43.53	27.23	19.20	21.43	23.66	25.89	37.50	78.57	98.99
LDeP 3rd order(IFS)	95.76	95.76	64.96	57.14	49.11	45.98	49.33	53.57	64.96	67.85	64.96	54.46	54.46	48.21	50.45	55.13	64.96	94.20	99.33
Improvement (%)	19.16	19.16	78.56	100.0	92.97	82.32	108.5	81.84	61.67	16.90	49.23	100.0	183.6	124.9	113.2	112.9	73.23	19.89	0.34

Fig. 7. Comparison between the different rotation angles of the IFS-based and non-IFS-based to LDeP 3rd order method

6.2 Analysis on Scale

Experimental data. For the analysis of scale robustness, all 112 texture images are scaled with scaling factors of 0.5 to 1.5 with 0.1 intervals (11 scales for each image). Here we use the bicubic interpolation and antialiasing methods for scaling of image. Each scaled image is divided into four non-overlapping 320×320 sub-images. Four 128×128 sub-images are then cropped from the center of the 320×320 sub-images. Hence, we obtain a scaled test set with 4,928 (=112×11×4) sub-images. Fig. 8 shows an example in different scale factors: 0.5, 0.6, 0.8, 1.0, 1.2, 1.3, 1.4, and 1.5.

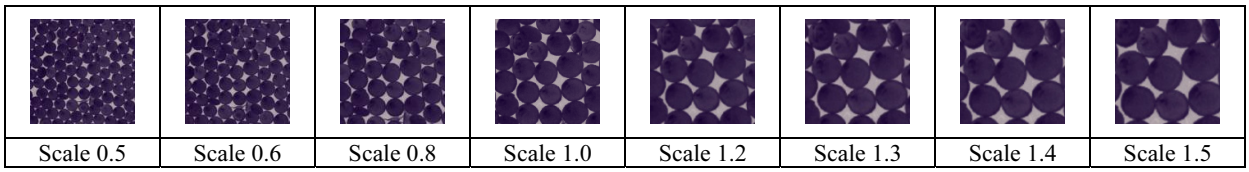

Scale 0.5	Scale 0.6	Scale 0.8	Scale 1.0	Scale 1.2	Scale 1.3	Scale 1.4	Scale 1.5

Fig. 8. Example scaled test set for image D66 from the CBT database; scale factors are 0.5, 0.6, 0.8, 1.0, 1.2, 1.3, 1.4 and 1.5

Experimental setup. We also use 1-NN approach as a classifier. The sample data was split into training and test sets using the 25-fold cross-validation method.
Experimental results. The results of classification accuracy with respect to scale factors for six tested methods are shown in Fig. 9 for clear comparison, and we also explore the IFS-based methods are more effective classification than non-IFS-based methods under multi-scale factors. That confirms the robustness of IFS-based methods. In addition, Table 3 represents the average accuracy rate of all scale factors on the CBT database and the average improvement rate after using IFS. It can also be seen from the table that the average improvement rate is significantly increased after using IFS-based method.

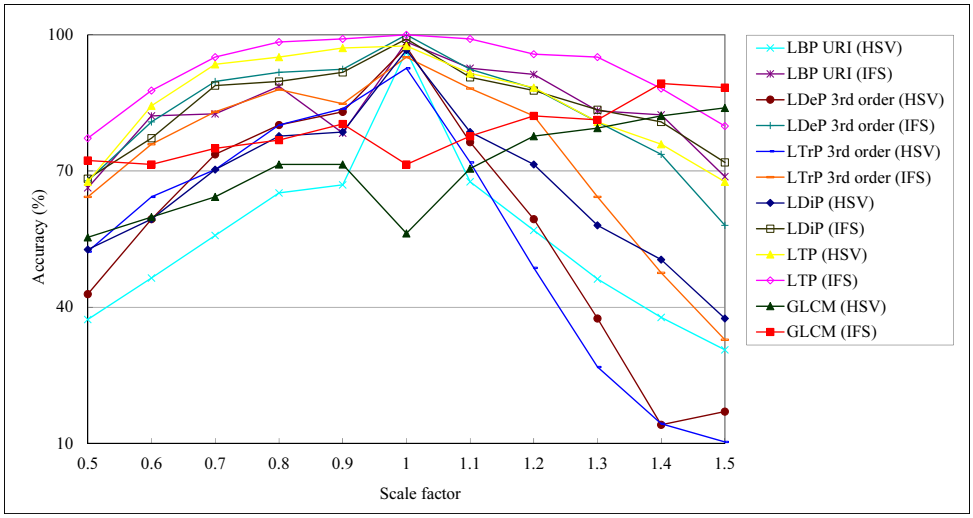

Fig. 9. Texture classification results for six tested methods with IFS-based and non-IFS-based on the scaled CBT database

Table 3. Average accuracy rate of all scale factors and the average improvement rate of performance after using IFS

Method	LBP_{URI}		GLCM		LTP		LDiP		LDeP		LTrP	
	HSV	IFS	HSV	IFS	HSV	IFS	HSV	IFS	HSV	IFS	HSV	IFS
Average accuracy rate (%)	55.19	83.16	70.21	78.73	85.41	92.33	66.48	84.50	58.24	83.24	55.93	73.28
Average improvement rate (%)	50.66		12.14		8.10		27.10		42.92		31.02	

Furthermore, the LBP_{URI} method in Table 3 has the best average improvement rate, and uses the red line in Fig. 10 to show its accuracy improvement rate after using IFS at each scale factor. We can see that there is significant improvement to gain at certain scale factor. Besides, we also summarize the accuracy above 90% for six tested methods. It is also found that IFS-based methods still can improve the accuracy from 0.88% to 8.29% even under high accuracy. The average improvement rate of accuracy can reach 2.99%.

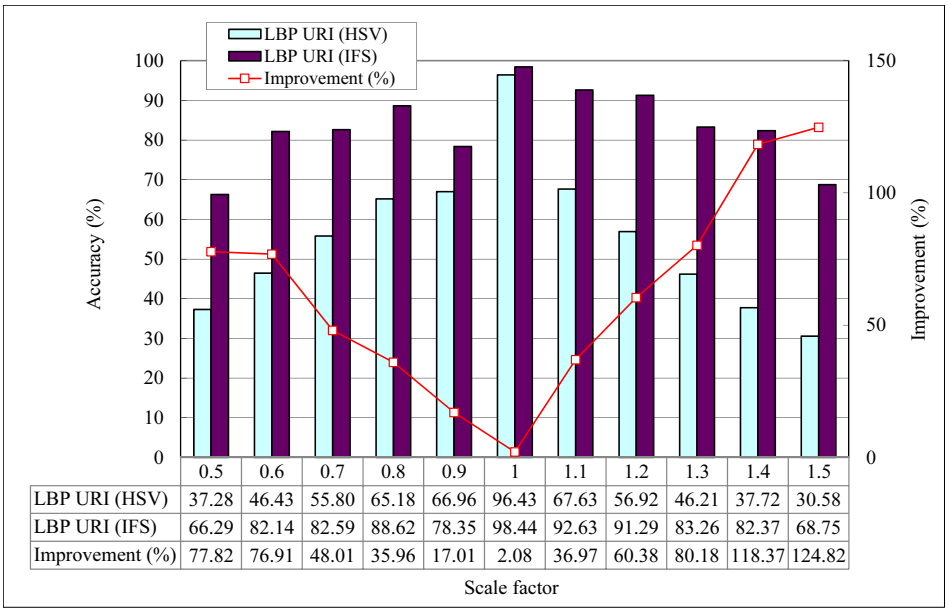

	0.5	0.6	0.7	0.8	0.9	1	1.1	1.2	1.3	1.4	1.5
LBP URI (HSV)	37.28	46.43	55.80	65.18	66.96	96.43	67.63	56.92	46.21	37.72	30.58
LBP URI (IFS)	66.29	82.14	82.59	88.62	78.35	98.44	92.63	91.29	83.26	82.37	68.75
Improvement (%)	77.82	76.91	48.01	35.96	17.01	2.08	36.97	60.38	80.18	118.37	124.82

Fig. 10. Comparison between the different scale factors of the IFS-based and non-IFS-based to LBP_{URI} method

7 Conclusions

In this paper, we found the IFS-based methods always achieve higher accuracy than non-IFS-based methods for six well-known texture descriptors, namely LBP, GLCM, LTP, LDiP, LDeP and LTrP. The accuracy is improved from 0.88% to 13.16%. Additionally, it is evident that IFS-based methods still can improve the accuracy even under high accuracy above 90% for robustness to rotation and scale, the average improvement rate of accuracy can reach 3.28% and 2.99% respectively. The above description shows that the IFS-based approach can improve the performance and robustness of existing texture classification techniques. And the conclusions can be used by texture classification researchers to further improve the performance of their own texture classification methods. In addition, because IFS-based methods are so clearly more effective at color texture classification than non-IFS-based methods—even after images are changed in rotation and scale—we will conduct an extended study on analyzing whether the limitations on the use of IFS-based methods and employing on applications in the future, such as the recognition of medical images, biometrics, ears, eyes, faces, gait, fingerprints, video, aerial photography, satellite imagery, and so forth.

References

[1] H.H. Anne, Texture Feature Extraction Methods: A Survey, IEEE Access 7(2019) 8975-9000.

[2] K.T. Atanassov, Intuitionistic fuzzy sets, Fuzzy Sets and Systems 20(1)(1986) 87-96.

[3] T. Tirupal, B.C. Mohan, S.S. Kumar, Multimodal medical image fusion based on Yager's intuitionistic fuzzy sets, Iranian Journal of Fuzzy Systems 16(1)(2019) 33-48.

[4] F. Zhao, H. Liu, J. Fan, C. Chen, R. Lan, N. Li, Intuitionistic fuzzy set approach to multi-objective evolutionary clustering with multiple spatial information for image segmentation, Neurocomputing 312(2018) 296-309.

[5] S.V. Aruna Kumar, B.S. Harish, A modified intuitionistic fuzzy clustering algorithm for medical image segmentation, Journal of Intelligent Systems 27(4)(2017).

[6] A.K. Singh, D. Choudhary, S. Tiwari, Feature extraction and classification methods of texture images: Performance analysis of feature extraction methods under different classifiers, LAP LAMBERT Academic Publishing, 2013.

[7] R.M. Haralick, K. Shanmugam, I. Dinstein, Textural features for image classification, IEEE Transactions on Systems, Man, and Cybernetics SMC-3(6)(1973) 610-621.

[8] F.R.D. Siqueira, W.R. Schwartz, H. Pedrini, Multi-scale graylevel co-occurrence matrices for texture description, Neurocomputing 120(2013) 336-345.

[9] J.H. Kim, S.C. Kim, T.J. Kang, Fractal dimension co-occurrence matrix method for texture classification, in Proc. of TENCON 2006 - IEEE Region 10 Conference, 2006.

[10] A.R. Mamat, M.K. Awang, N.A. Rawi, M.I. Awang, M.F.A. Kadir, Average analysis method in selecting Haralick's texture features on color co-occurrence matrix for texture based image retrieval, International Journal of Multimedia and Ubiquitous Engineering 11(2)(2016) 79-88.

[11] T. Ojala, M. Pietikäinen, D. Harwood, A comparative study of texture measures with classification based on feature distributions, Pattern Recognition 29(1)(1996) 51-59.

[12] X. Tan, B. Triggs, Enhanced local texture feature sets for face recognition under difficult lighting conditions, Analysis and Modelling of Faces and Gestures, Lecture Notes Computer Science 4778(2007) 168-182.

[13] B. Jun, T. Kim, D. Kim, A compact local binary pattern using maximization of mutual information for face analysis, Pattern Recognition 44(3)(2011) 532-543.

[14] T. Jabid, M.H. Kabir, O. Chae, Local directional pattern (LDP) for face recognition, in Proc. IEEE International Conference of Consumer Electronics, 2010.

[15] B. Zhang, Y. Gao, S. Zhao, J. Liu, Local derivative pattern versus local binary pattern: Face recognition with high-order local pattern descriptor, IEEE Transactions on Image Processing 19(2)(2010) 533-544.

[16] S. Murala, R.P. Maheshwari, R. Balasubramanian, Local tetra patterns: A new feature descriptor for content-based image retrieval, IEEE Transactions on Image Processing 21(5)(2012) 2874-2886.

[17] S.R. Dubey, S.K. Singh, R.K. Singh, Local bit-plane decoded pattern: a novel feature descriptor for biomedical image retrieval, IEEE Journal of Biomedical and Health Informatics 20(4)(2016) 1139-1147.

[18] M. Verma, B. Raman, Local neighborhood difference pattern: a new feature descriptor for natural and texture image retrieval, Multimedia Tools and Applications 77(10)(2018) 11843-11866.

[19] P. Banerjee, A.K. Bhunia, A. Bhattacharyya, P.P. Roy, S. Murala, Local neighborhood intensity pattern – a new texture feature descriptor for image retrieval, Expert Systems with Applications 113(2018) 100-115.

[20] P. Muthukumar, G.S.S. Krishnan, A similarity measure of intuitionistic fuzzy soft sets and its application in medical diagnosis, Applied Soft Computing 41(2016) 148-156.

[21] H. Nguyen, A novel similarity/dissimilarity measure for intuitionistic fuzzy sets and its application in pattern recognition, Expert Systems with Applications 45(2016) 97-107.

[22] V.P. Ananthi, P. Balasubramaniam, A new image denoising method using interval-valued intuitionistic fuzzy sets for the removal of impulse noise, Signal Processing 121(2016) 81-93.

[23] H. Nguyen, A new knowledge-based measure for intuitionistic fuzzy sets and its application in multiple attribute group decision making, Expert Systems with Applications 42(22)(2015) 8766-8774.

[24] I.K. Vlachos, G.D. Sergiadis, Intuitionistic fuzzy information: applications to pattern recognition, Pattern Recognition Letters 28(2)(2007) 197-206.

[25] I.K. Vlachos, G.D. Sergiadis, Intuitionistic Fuzzy Image Processing, in: Proc. Encyclopedia of Artificial Intelligence, 2009.

[26] M. Sugeno, Fuzzy measures and fuzzy integrals: a survey, in: M.M. Gupta, G.N. Saridis, B.R. Gaines (Eds.), Fuzzy Automata and Decision Processes, North Holland, 1977, pp. 89-102.

[27] C.E. Shannon, A mathematical theory of communication, The Bell System Technical Journal 27(1948) 379-423.

[28] A.D. Luca, S. Termini, A definition of a nonprobabilistic entropy in the setting of fuzzy sets theory, Information and Control 20(4)(1972) 301-312.

[29] R.C. Gonzales, R.E. Woods, Digital Image Processing, third ed., Prentice-Hall, 2008.

[30] E. Szmidt, J. Kacprzyk, Distances between intuitionistic fuzzy sets, Fuzzy Sets and Systems 114(3)(2000) 505-518.

[31] Z. Liang, P. Shi, Similarity measures on intuitionistic fuzzy sets, Pattern Recognition Letters 24(15)(2003) 2687-2693.

[32] H.B. Mitchell, On the Dengfeng–Chuntian similarity measure and its application to pattern recognition, Pattern Recognition Letters 24(16)(2003) 3101-3104.

[33] P. Julian, T. Hung, S. Lin, On the Mitchell similarity measure and its application to pattern recognition, Pattern Recognition Letters 33(9)(2012) 1219-1223.

[34] B. Pekala, K. Balicki, Interval-valued intuitionistic fuzzy sets and similarity measure, Iranian Journal of Fuzzy Systems 14(4)(2017) 87-98.

[35] W. Kabsch, A solution for the best rotation to relate two sets of vectors, Acta Crystallographica Section A 32(5)(1976) 922-923.